Enrichment of Retinal Ganglion Cells in Rat Retinal Lysate by Excimer Laser Ablation of the Outer Retina

Christian van Oterendorp,[1,2] *Wolf A. Lagrèze,*[2] *Eva-Maria Gutekunst,*[2] *Stavros Sgouris,*[2,3] *Philip Maier,*[2] *and Julia Biermann*[2]

Purpose. Retinal ganglion cells (RGC) are a relatively small cell population in the retina. This leads to an unfavorable signal-to-noise ratio when analyzing RGC proteins in whole retina lysate. We present a novel technique to obtain RGC-enriched rat retinal lysate by removing the outer retinal layers with an excimer laser before lysation.

Methods. Outer retinal layers were ablated with an excimer laser on flat mounted retinas from adult albino rats. 4′6-Diamidino-2-phenylindole dihydrochloride hydrate (DAPI) nuclear staining was used to assess the ablation efficacy ($n = 6$). Western blot for layer specific markers (rhodopsin, parvalbumin, β-III-tubulin) was performed to quantify changes in protein composition ($n = 7$). Excimer-ablated (EX) and full-thickness (FT) retinas 48 hours after optic nerve crush (ONC) were compared regarding the effect on phospho–cAMP response element binding protein (pCREB) and Thy1 levels ($n = 5$).

Results. Area quantification of DAPI-stained retinas showed that 73% ± 4.9% of the ablation area was free of photoreceptor and bipolar cell nuclei. In Western blot, laser ablation led to a significant reduction of the photoreceptor marker rhodopsin and increase of the ganglion cell layer (GCL) marker β-III–tubulin (relative quantity: rhodopsin 0.47 ± 0.05, $P < 0.0001$; β-III–tubulin 2.35 ± 0.37, $P = 0.02$). Changes of pCREB and Thy1 after ONC were significantly different between FT and EX retinas (relative quantity pCREB: FT 1.4 ± 0.16, EX 0.78 ± 0.07, $P = 0.008$; Thy1: FT 0.95 ± 0.02, EX 0.63 ± 0.07, $P = 0.006$).

Conclusions. We demonstrated that excimer laser ablation of outer retinal layers is feasible, producing RGC-enriched retinal lysate. Laser ablation may allow a more specific detection of RGC responses to experimental stimuli. (*Invest Ophthalmol Vis Sci.* 2013;54:2061–2067) DOI:10.1167/iovs.12-11389

Retinal ganglion cells (RGC) are a relatively small population in the retina. In rats, they comprise approximately 100,000 cells[1] compared to a total of approximately 5,000,000 retinal cells (2%). This leads to an unfavorable signal-to-noise ratio when analyzing RGC proteins in whole retinal lysate. Thus, small changes of RGC proteins may be missed. Results could even be misleading if another cell population, such as glia cells, responds differently.

Various attempts have been made to overcome this problem by targeted sampling of the inner retina or even single RGCs. Among those techniques laser capture microscopy is well established[2–4] allowing a precise dissection of cell layers or cell bodies from tissue sections. However, the amount of material that can be obtained is very small, sufficient only for RNA analyses, but not for protein quantification by Western blot or ELISA.

An approach providing larger amounts of cell material is immunopanning.[5–7] RGCs from enzymatically dissociated retinas are immobilized to a solid surface by use of RGC specific antibodies. After washing away the nonadherent cells the immobilized RGCs can be lysed and subjected to protein analysis. Major limitations of this method are the rather low yield of RGCs and the relatively long time from axon injuring explantation to lysation of the cells of at least 20 minutes. During this time early response signaling cascades already may be activated, potentially altering the posttranslational modification (mainly phosphorylation) and/or the amount of proteins with high turnover.

A different approach has been named retinal shaving. Until the present, to our knowledge there exists only one report[8] on this technique that uses mechanical shaving of the outer retina to reduce the content of photoreceptor and bipolar cell proteins in retinal lysate. The precision and reliability of this method remain unclear from the original publication, and this appears to be a major limitation of this method.

The excimer laser allows a depth-controlled ablation of tissue without significant thermal damage.[9,10] It is used widely in corneal refractive surgery.[11] Due to its physical principle, the original contour of the tissue surface is retained. However, due to tissue inhomogeneity, laser ablation can produce a rough surface, which can be smoothened by use of masking substances, such as water or hyaluronic acid solutions.

We report on a novel technique to produce RGC-enriched rat retinal lysate by ablation of the outer retina with an excimer laser.

Materials and Methods

Animals Used

All animals used in this study were treated in accordance with the ARVO Statement for the Use of Animals in Ophthalmic and Vision Research. The protocols were approved by the Commission on the Use of Animals in Scientific Procedures of the local government (Tierversuchskommission, Regierungspräsidium, Freiburg, Germany; permit number G-10/106). All animals used were adult albino rats (Sprague-Dawley), weight 250 to 300 g.

From the [1]Department of Ophthalmology, Georg-August University Hospital Göttingen, Germany; [2]University Eye Hospital Freiburg, Germany; and the [3]Department of Ophthalmology, Johannes Gutenberg University Medical Center, Mainz, Germany.

Submitted for publication November 27, 2012; revised January 24, 2013; accepted February 20, 2013.

Disclosure: **C. van Oterendorp**, None; **W.A. Lagrèze**, None; **E.-M. Gutekunst**, None; **S. Sgouris**, None; **P. Maier**, None; **J. Biermann**, None

Corresponding author: Christian van Oterendorp, Department of Ophthalmology, Georg-August University Hospital Göttingen, Robert-Koch-Strasse 40, 37075 Göttingen, Germany; christian.oterendorp@med.uni-goettingen.de.

Preparation, Laser Treatment, and Lysation of the Retina

The retina was explanted from the eyeball in ice-cold Hank's balanced salt solution (HBSS) and flat mounted on a custom made rigid contact lens (material polyvinyl chloride, diameter 15 mm, radius of curvature 8.5 mm) with the RGCs facing down (Fig. 1A). Several drops of ice-cold methanol were applied to start tissue fixation immediately and a second contact lens was mounted on top to smoothen the outer retinal surface (Fig. 1B). The sandwich was placed in an approximately 5 mm deep bath of ice-cold methanol for 10 minutes to ensure homogeneous fixation. Before laser treatment, the second contact lens was removed.

Laser ablation (Fig. 1C) was performed with an excimer laser (Schwind Amaris; Schwind, Kleinostheim Germany) using the built-in phototherapeutic keratectomy program. Laser ablation was performed as a two-step procedure. For the first step, the depth of ablation was set to 95 μm and 0.25% hyaluronic acid eye drops (LaserVis; TRB Chemedica, Haar, Germany) were used as masking substance. The second step was performed with 20 μm depth of ablation, using methanol as masking substance. Further laser settings were: diameter of the treatment area 7 mm, radius of curvature 30 diopters. The field of ablation was centered to the optic nerve head. The small rim of nonablated peripheral retina remaining after the treatment (Fig. 2E) was cut off with a scalpel. For lysation, the retina was peeled off the contact lens, transferred to 70 μL of radioimmunoprecipitation assay (RIPA) lysis buffer (150 mM NaCl, 1.0% NP-40, 0.5% sodium-deoxycholate, 0.1% SDS, 50 mM Tris-Cl, pH 8.0; protease inhibitor cocktail; Complete mini, Roche, Germany; and phosphatase inhibitor 200 μM sodium orthovanadate; Sigma-Aldrich, Munich, Germany) and lysed thoroughly with an ultrasound probe (Bandelin Sonopuls, Berlin, Germany).

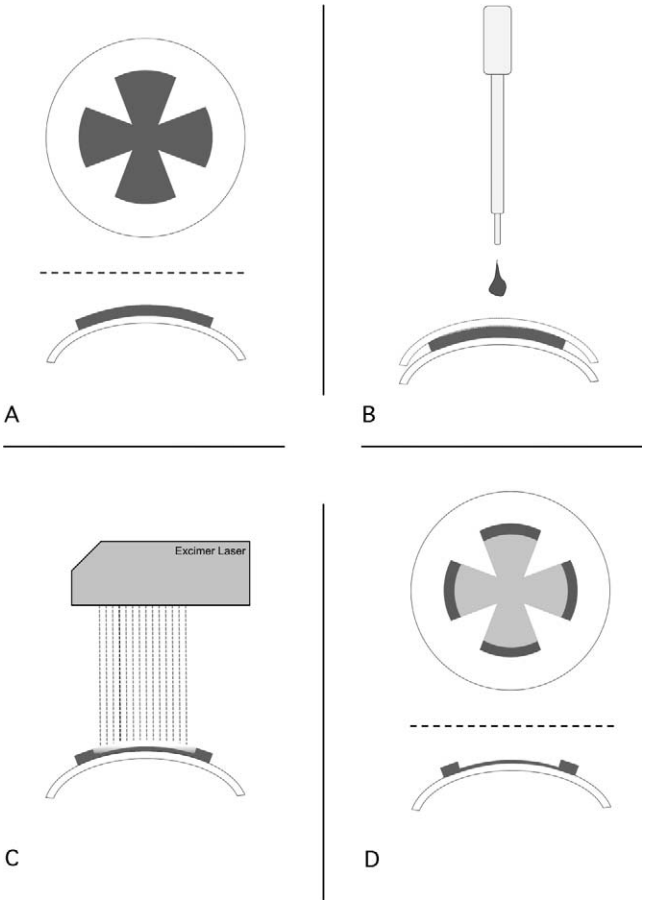

Figure 1. Schematic illustration of the laser ablation protocol. (**A**) Flat mount of the retina with the GCL facing down on a large rigid contact lens shown from *top* and *side* view. (**B**) Fixation of the retina with several drops of ice-cold methanol, followed by placement of a second contact lens to smoothen the surface. The sandwich then is placed in a shallow bath of ice cold methanol for 10 minutes. (**C**) Laser ablation of a 7-mm circular area after removal of the upper contact lens. Use of hyaluronic acid eye drops and methanol as masking substances. (**D**) Laser-ablated retina with the small rim of nonablated peripheral retina (*dark gray*) shown from *top* and *side*. For tissue lysis, the nonablated rim was excised, and the remaining retina peeled off the contact lens and subjected to lysis by ultrasound.

Fluorescence Microscopy of the Flat Mounted Retina

For evaluation of the laser ablation before tissue lysis, the retina was left on the contact lens after ablation. A second contact lens was mounted again using Mowiol mounting medium (Calbiochem, San Diego, CA) containing 1:10,000 4′,6-diamino-2-phenylindole dihydrochloride hydrate (DAPI; Sigma) for nuclear staining.

The whole retina was serially photographed with a fluorescence microscope (Zeiss AxioImager A1; Zeiss, Oberkochen, Germany) at ×100 magnification. The serial images were merged to a single image with the MosaicJ plug-in of ImageJ software (available in the public domain at http://imagej.nih.gov/ij). As the three nuclear layers of the retina are distinguishable by the average size and density of their nuclei, the DAPI images of the flat mount allowed an approximate evaluation of the laser ablation efficiency (Fig. 2F, see Supplementary Material and Supplementary Video S1, http://www.iovs.org/lookup/suppl/doi:10.1167/iovs.12-11389/-/DCSupplemental).

Quantification of the outer retina islets (inner and outer nuclear layers) remaining after laser ablation was performed with ImageJ software by manual delineation of the specific areas. Results were presented as mean ± SEM. Bonferroni-Holm correction for multiple comparisons was applied.

Optic Nerve Crush (ONC)

ONC was performed as described previously.[12] Briefly, rats were anesthetized with isoflurane. The orbit was opened through an incision at the superior orbital rim and the optic nerve was approached by partially resecting the lacrimal gland. The optic nerve sheath was cut open longitudinally 1 to 2 mm posterior to the globe, while care was taken not to damage blood vessels. The optic nerve was crushed with blunt forceps for 10 seconds. Before wound closure, the retinal perfusion was ascertained funduscopically. Animals with severe reduction of perfusion were excluded.

Cryosectioning and Immunohistochemistry

For evaluation of the retinal morphology after laser ablation the flat mounted retinas were fixated with 4% paraformaldehyde solution for 1 hour, followed by immersion in 30% sucrose solution for one additional hour. The fixated retina was peeled off the glass slide, embedded in OCT medium, cryosectioned to 10 μm, and stained with hematoxylin and eosin (H&E).

For immunohistochemistry of retinal layer markers whole eyes were used. Fixation and sucrose treatment were performed as described above with an incubation time of 4 hours for each step. The eyes were embedded in OCT medium and cryosectioned to 10 μm. For immunostaining the sections were blocked with 5% BSA, 0.3% Triton in PBS solution at room temperature for 10 minutes. The first antibody was applied in blocking buffer, the second antibody (Alexa-488 or -568 conjugated; Invitrogen/Life Technologies, Darmstadt, Germany) diluted 1:1000 in PBS. First antibodies used were: rhodopsin 1:100 (Abcam, Cambridge, UK), parvalbumin 1:500 (Sigma-Aldrich),

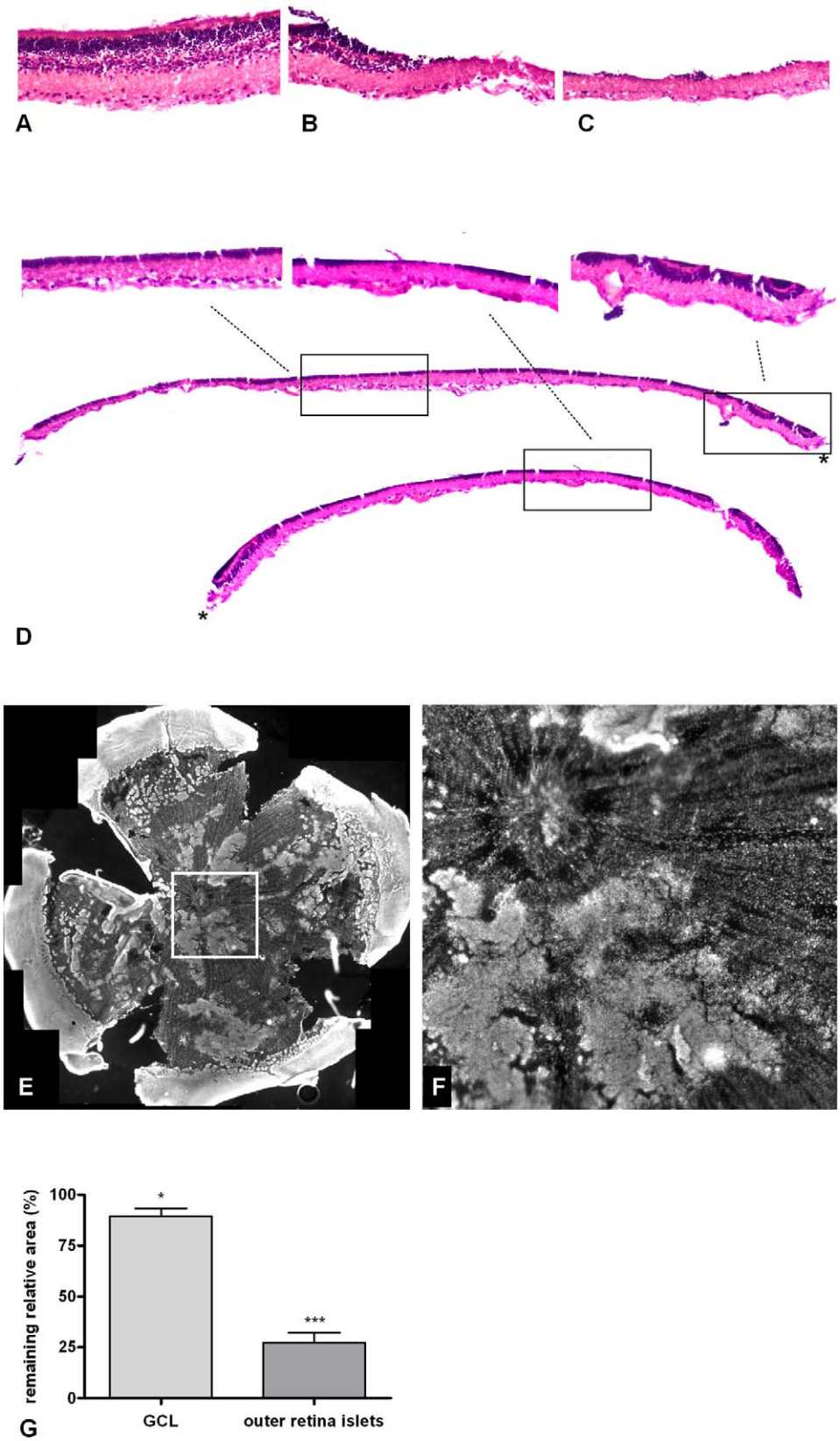

Figure 2. Retinal morphology after laser ablation. (**A–D**) H&E stained cryosections of retinas ablated without methanol fixation and 100 μm ablation depth to study the effect of the laser ablation on the soft retinal tissue. In all images the GCL is facing *down*. Magnification is ×200. The laser produced a relatively sharp edge, particularly in the nuclear layers, without apparent damage to the surrounding tissue. (**A**) Nonablated peripheral retina. (**B**) Transition zone between ablated and FT retina. (**C**) Ablated retina. (**D**) Continuous longer segments of ablated retina with magnified insets. Both segments are from the same histologic section. The ends marked with *asterisks* were adjacent in the original section. (**E**, **F**) Representative en face image of a DAPI stained retinal flat mount after ablation following the final laser protocol described in the Materials and

Methods section. The *white square* in (**E**) delineates the area further magnified in (**F**). Note the difference between the radially arranged RGCs with larger nuclei and the brighter-appearing outer retina islets comprising mainly of inner nuclear layer nuclei. (**G**) Quantification of the postlaser GCL area (*left bar*) and the ORI area (*right bar*) in six consecutively-treated retinas. The postlaser GCL area is given as percentage relative to the prelaser area of the flat mounted retina. The area outside the 7 mm ablation zone was not taken into account. The ORI area was calculated as percentage relative to the postlaser GCL area. The difference to the value 1 (no difference to the respective reference area) was statistically significant for both parameters ($P = 0.04$ for GCL area, $P < 0.0001$ for ORI).

and β-III–tubulin 1:5000 (Promega, Mannheim, Germany). Images were processed with ImageJ software. No nonlinear adjustments were made.

SDS-PAGE and Western Blotting

Retinas were ablated following the protocol described above. The FT retinas underwent the same flat mounting and methanol fixation step, and subsequently were trephined to 7 mm diameter to match the area of laser ablation. For each retinal lysate two separate Western blots were run and the results were averaged.

SDS-PAGE and Western blots were performed following standard protocols. Briefly, proteins were separated on a 10% acrylamide SDS gel followed by protein transfer onto a PVDF membrane (Immobilon-P; GE Healthcare, Munich, Germany) by wet blotting. The membrane was blocked in 5% BSA in TBS-Tween 0.1% (TBS-T) solution for 60 minutes at room temperature. First antibodies were diluted in blocking buffer and incubated overnight at 4° Celsius. The antibodies used were: rhodopsin 1:2000 (Abcam), parvalbumin 1:2000 (Sigma-Aldrich), β-III–tubulin 1:10,000 (Promega), Thy1 1:10,000 (AbD Serotec, Düsseldorf, Germany), phospho–cAMP response element binding protein (pCREB) 1:1000 (Cell Signaling/New England Biolabs, Frankfurt, Germany), β-actin 1:20,000 (Abcam), and glyceraldehyde-3-phosphate dehydrogenase (GAPDH) 1:20,000 (Millipore, Darmstadt, Germany). Secondary antibodies were horseradish-peroxidase conjugated anti-rabbit or anti-mouse IgG (Amersham ECL; GE Healthcare), diluted 1:20,000 in TBS-T. Protein bands were visualized with chemiluminescent reaction (ECL-Prime kit; GE Healthcare) and scanned with an electronic gel documentation system (ChemoCam; Intas, Göttingen, Germany).

Quantification of band intensity was performed with the ImageJ gel analyzer plug-in.

All band intensities were normalized to β-actin. To gain a more stable normalization parameter for the ONC experiments, GAPDH was used additionally and the geometric mean of both proteins was used as normalization value as proposed previously.[13] Results were presented as mean ± SEM. Bonferroni-Holm correction for multiple comparisons was applied.

Results

Retinal Morphology after Laser Ablation

The commercial excimer laser used in this project is designed primarily for the ablation of corneal tissue. Therefore, we first evaluated the laser effect on retinal tissue morphology. On flat mounted, unfixated retinas the ablation left a relatively sharp and smooth edge, particularly in the nuclear layers (Figs. 2B, 2D). The underlying tissue appeared undamaged (Figs. 2B–D). Through variation of the laser settings and the number of laser cycles applied, the overall depth of ablation could be adjusted. A certain variation of the ablation depth inside the treatment area always was present (see Supplementary Material and Supplementary Video S1, http://www.iovs.org/lookup/suppl/doi:10.1167/iovs.12-11389/-/DCSupplemental), but could be reduced significantly through introduction of specific features to the laser protocol as illustrated in Figure 1. They include the use of a rigid contact lens for mounting the retina, short methanol fixation of the tissue, a two-step ablation, and the use of masking substances (for details see Materials and Methods section and Fig. 1). Thus, a more efficient ablation of the outer retina (arbitrarily defined as retinal layers peripheral to the ganglion cell layer [GCL]) and better preservation of the inner retina (nerve fiber layer [NFL] and GCL) was obtained. However, given the very thin border between the layers to be removed and preserved, a trade-off between allowing remnants of the outer retina and reducing damage to the GCL was unavoidable. Aiming for a maximum yield of RGCs we set the laser energy such that GCL damage was minimized and remnant islets of outer retina cells (Figs. 2E, 2F) were accepted to a certain degree.

An evaluation of the ablation during the laser procedure technically was not feasible. This, unfortunately, ruled out the possibility of a targeted relasering of remaining outer retina

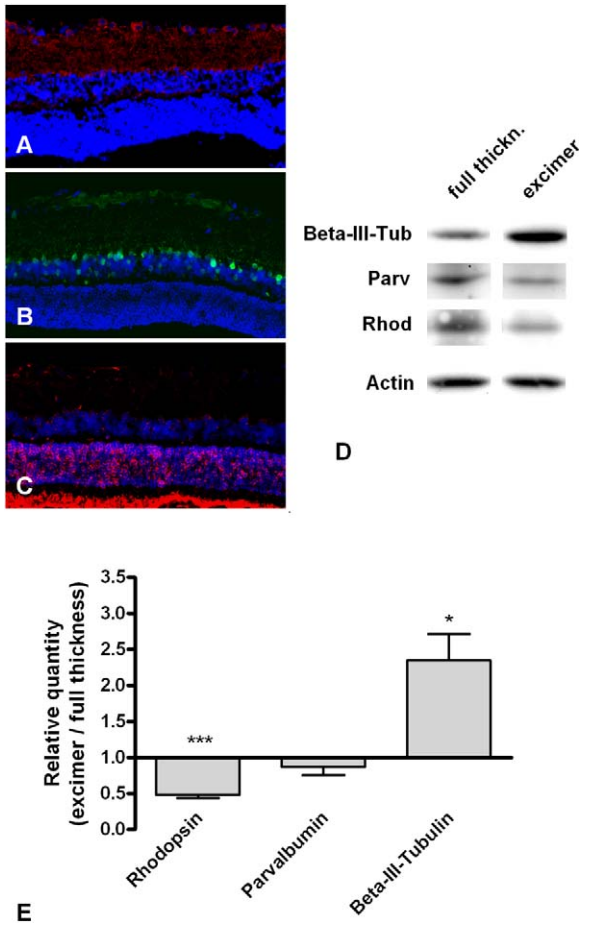

Figure 3. Changes of retinal layer markers after laser ablation. (**A–C**) Anatomic distribution of the marker proteins used. All images are composite images of the marker protein (*red* or *green*) and the DAPI-stained nuclei (*blue*) with the GCL facing *up*. (**A**) β-III–tubulin. (**B**) Parvalbumin. (**C**) Rhodopsin. (**D**) Representative Western blots of the marker proteins as analyzed from FT or EX retinas. (**E**) Quantitative analysis of Western blots. The marker protein band intensities were normalized to β-actin, and expressed as ratio between EX and FT samples. A ratio <1 indicates a loss of marker protein due to laser ablation, while a ratio >1 indicates an enrichment of a marker protein. A significant loss of rhodopsin and enrichment of β-III–tubulin after laser ablation was detected ($n = 7$ for each group).

islets. Therefore, we developed a method for a quick postlaser evaluation before subjecting the retina to lysation. Thus, information on the ablation quality of each retina could be obtained and retinas with an unsatisfactory laser ablation may be discarded before selecting them for protein analyses. The evaluation method was based on a nuclear staining with DAPI, which was applied to the laser ablated flat mounted retina. The characteristic size and density of the nuclei allowed for an identification of the three nuclear layers (Fig. 2F, Supplementary Material and Supplementary Video S1, http://www.iovs.org/lookup/suppl/doi:10.1167/iovs.12-11389/-/DCSupplemental). The GCL is characterized by large nuclei and large internuclear spaces, while the outer nuclear layer exhibits small and densely packed nuclei. The inner nuclear layer shows an intermediate pattern.

Within the treatment zone, we quantified the area where GCL nuclei were present, including the areas of overlying outer retina islets, and termed it postlaser GCL area. Secondly, the total area of remaining outer retina islets (termed ORI area) was determined. In a series of 6 consecutively ablated retinas the percentage of ORI area relative to the postlaser GCL area was 27% ± 4.9% ($P < 0.0001$, one sample *t*-test against the value 1). The percentage of the post-laser GCL area relative to the prelaser retinal flat mount area was 89% ± 3.9% ($P = 0.04$, Fig. 2G, the retina outside the treatment area was not included).

Changes of Retinal Layer Markers in Western Blot after Laser Ablation

To quantify the changes in retinal lysate protein composition after laser ablation, marker proteins specific for retinal layers were analyzed in Western blot. They included rhodopsin for the outer nuclear layer, parvalbumin for the inner nuclear layer and β-III–tubulin for the GCL. The anatomic distribution of the marker proteins in the retina is shown in Figures 3A to 3C.

Representative images of the protein bands in Western blot are shown in Figure 3D. For quantification of the difference between laser ablated and FT retinas, the ratio between the two groups was calculated ($n = 7$ for each group, Fig. 3E). A ratio of >1 signifies an enrichment of a marker protein, a ratio of <1 a loss of the protein. The results for the analyzed layer markers were rhodopsin 0.47 ± 0.05 ($P < 0.0001$, one sample *t*-test against the value 1 with Bonferroni-Holm correction for multiple comparison), parvalbumin 0.87 ± 0.11 ($P = 0.3$), and β-III–tubulin 2.35 ± 0.37 ($P = 0.02$). In summary, laser ablation leads to a significant reduction of photoreceptor proteins and an enrichment of RGC proteins. Parvalbumin as a protein of GCL neighboring cells shows a trend towards lower levels compared to FT retinal lysate.

Differences between Ablated and FT Retinas in pCREB and Thy1 Levels after ONC

Using laser ablation, we aimed for a higher sensitivity and specificity in detecting RGC responses to optic nerve diseases. To test whether the method, indeed, provides significantly different results compared to FT retinal lysate, we performed an ONC as a model of an acute, highly synchronized RGC injury. The animals were assigned randomly to provide either laser ablated or FT retinal lysate for analysis in Western blot ($n = 5$ for each group). pCREB and Thy1 were chosen as proteins of interest.

pCREB is a downstream target of the axonal neurotrophic signaling cascade, mediating neuronal survival. It is expressed in the GCL and the inner nuclear layer. As a consequence of the ONC-induced breakdown of the axonal neurotrophic signaling cascade, pCREB levels have been shown to decrease in RGCs.[14] However, triggered by the acute neurodegeneration

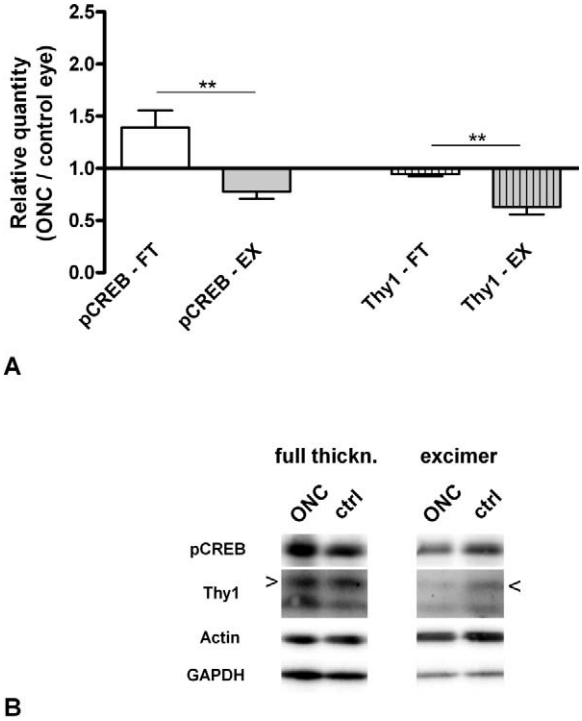

Figure 4. Difference in detecting the response to ONC (48-hour time point) between FT and laser ablated retinas. (**A**) Quantitative Western blot data for pCREB (*left two bars*) and Thy1 (*right two bars*). Each *bar* shows the ratio between ONC and control eye. Ratio <1 indicates reduced levels of the protein after ONC, ratio >1 elevated levels. Laser ablation (EX) led to significantly different results compared to FT lysate for both proteins analyzed ($n = 5$ for each group). (**B**) Representative Western blots. Note the *arrow* in the second row pointing to the Thy 1 band. The *left two columns* show ONC and control eye pairs analyzed from FT retinas. The *right two columns* show the laser-ablated sample pairs. β-Actin and GAPDH were used for normalization of the quantitative data.

non-RGC retinal cells may be activated and exhibit elevated pCREB levels. When analyzing FT retinal lysate 48 hours after ONC (Fig. 4), pCREB levels were, indeed, slightly elevated (1.4 ± 0.16, mean ± SEM). In contrast, analysis of laser ablated retinal lysate showed a decrease of pCREB (0.78 ± 0.07). The difference between both groups was statistically significant ($P = 0.008$; 2-tailed *t*-test with Bonferroni-Holm correction for multiple comparison).

Thy1 is a surface protein specific for RGCs. Injury of RGCs leads to a downregulation of Thy1.[15,16] In our experiments, analysis of FT retinal lysate 48 hours after ONC (Fig. 4) showed a weak trend towards lower Thy1 levels (0.95 ± 0.02). In lysate from laser ablated retinas the ONC response was more apparent (0.63 ± 0.07) and the difference to the FT group was statistically significant ($P = 0.006$, 2-tailed *t*-test with Bonferroni-Holm correction for multiple comparison).

For both proteins, laser ablation led to significantly different and pathophysiologically more appropriate results compared to the analysis of FT retinas.

Discussion

The aim of our work was to produce RGC-enriched retinal lysate for protein analyses by excimer laser ablation of the outer retina. Due to the principle of our method, the remaining tissue is "contaminated" with non-RGC cells. They firstly encompass micro- and astroglia of the NFL and GCL, as well as Müller cell end feet extending to the inner retina. Secondly,

islets of inner and outer nuclear layer cells remained after laser ablation as shown in Figures 2E to 2G. The latter cells may have been reduced by a more aggressive ablation protocol, but which in turn would have set the GCL at risk of being significantly ablated as well. Thus, our final laser protocol is a trade-off between maximized ablation of the outer retina and minimized loss of RGCs. Despite these limitations, the resulting lysate contains significantly more RGC protein (β-III–tubulin) and less photoreceptor protein (rhodopsin), which increases the chance of detecting RGC specific responses to experimental procedures.

In the ablation analyses shown in Figure 2G, almost three quarters of the preserved GCL area appeared free of inner and outer nuclear cell islets. Compared to this, the reduction in parvalbumin Western blot signal is relatively small (Fig. 3E). A possible explanation may be that parvalbumin-positive cells are located adjacent to or partially inside the GCL (Fig. 3B). Furthermore, the smaller lysis buffer volume used for the smaller tissue volume of the ablated retinas compared to FT samples leads to a relative concentration effect of the remaining parvalbumin-positive cells. Thus, the ablation of the inner nuclear layer may be more efficient than suggested by the parvalbumin Western blot signal.

Starting with preliminary experiments using unfixated retinas flat mounted on microscopy glass slides the laser protocol was modified to increase reliability and specificity of the ablation. Key parameters of the final protocol were the use of a rigid contact lens, a short methanol fixation of the retina, a two-step ablation, and the use of masking substances. Flat mounting the retina on a curved surface had two main advantages. The excimer laser, designed for corneal surgery, is not programmed for ablation of flat surfaces. Leaving the retina in a curved shape, thus, avoided an incorrect ablation at the periphery. Moreover, the curved surface led to a more even distribution of the masking substances, which on a flat surface tended to retain a drop-like shape due to their inherent surface tension.

A quick methanol fixation step was introduced to avoid protein degradation during the laser procedure and to make the tissue more resistant to ablation with higher laser energies. In unfixated retinas small differences in the time between death of the animal and start of the laser treatment caused a relatively large variation in ablation efficiency. Methanol fixation widens the postmortem time window for consistent laser ablation. Also, in combination with a second contact lens placed on top of the retina a much smoother outer retina surface can be created, which results in a more even ablation and, hence, better achievement of RGC preservation and outer retina elimination. The reduced protein yield when lysing fixated tissue could be minimized by using a sufficiently stringent lysis buffer formulation and an ultrasound probe (see Materials and Methods section).

Despite the use of masking substances, a single laser ablation still leaves a relatively uneven surface with a large number of outer retina islets. A second mild ablation step allows the repeated application of a masking substance to smoothen the surface. Further increasing the number of laser steps, however, resulted in larger variation of the total ablation depth. With the two ablation steps, the total time for the laser treatment was approximately 10 minutes. The time from excision of the retina to lysation (without DAPI staining) was approximately 20 to 25 minutes for each retina.

In theory, the excimer laser retains the contour of the outer tissue surface, which should lead to perfect results even in the presence of slight folds of the retinal flat mount. In reality, inhomogeneities of tissue hydration and fixation led to uneven surfaces with remaining islets of outer retinal cells. By use of masking substances the ablated surface was smoothened. To minimize the influence on the ablation depth low viscous substances were used: 0.25% hyaluronic acid eye drops for the first 95 μm step, and the very low viscous and highly volatile methanol for the 15 μm second ablation.

DAPI staining of the ablated flat mount allows an evaluation of the ablation efficacy under a fluorescence microscope. Visualizing only the three nuclear, but not the plexiform layers, the staining is fairly limited in its three-dimensional information. However, it is very quick to perform and still provides a good impression of the quality of ablation. It allows recognizing and discarding insufficiently ablated retinas, which helps to minimize the variability in retinal lysate protein composition introduced by the laser ablation itself.

To our knowledge, we report the first post-ONC pCREB Western blot analysis made from RGC-enriched lysate. The role of CREB as target protein of the axonal neurotrophic signaling cascade suggests a decrease in RGC-pCREB after ONC, which has been confirmed by Herdegen et al.[14] at a 5-day timepoint after ONC using immunohistochemistry. We attribute the increase of pCREB levels in FT retinal lysate to an ONC-induced glia activation.[17]

Thy1 is an RGC-specific protein known to be regulated sensitively in RGC injury. In a previous report, a drop in Thy1-mRNA levels was observed as early as 24 hours after ONC in mice.[15] The concomitant decrease in Thy1 protein level at 48 hours in our experiments could be detected only in excimer-ablated (EX) but not FT retinal lysate.

Shortcomings of our laser ablation technique are the additional time and the expensive laser needed. Compared to laser capture microscopy (LCM) the specificity of tissue dissection is inferior. However, unlike LCM, excimer laser ablation can provide amounts of tissue sufficient for Western blot or ELISA protein analyses.

In conclusion, our excimer laser ablation method produces RGC-enriched retinal lysate and allows detecting RGC specific signals that would have been lost in FT lysate.

For research on the outer retina, laser ablation may be applied to the inner retinal layers. However, the ablation protocol would have to be adapted.

Acknowledgments

The authors thank Sylvia Zeitler and Herbert Graner for excellent technical assistance, and Marie Follo for acquiring the confocal microscopy images.

References

1. Danias J, Shen F, Goldblum D, et al. Cytoarchitecture of the retinal ganglion cells in the rat. *Invest Ophthalmol Vis Sci*. 2002;43:587–594.
2. Curran S, McKay JA, McLeod HL, Murray GI. Laser capture microscopy. *Mol Pathol*. 2000;53:64–68.
3. van Oterendorp C, Lorber B, Jovanovic Z, Yeo G, Lagrèze WA, Martin KR. The expression of dynein light chain DYNLL1 (LC8-1) is persistently downregulated in glaucomatous rat retinal ganglion cells. *Exp Eye Res*. 2011;92:138–146.
4. Guo Y, Ceperna WO, Dyck JA, Doser TA, Johnson EC, Morrison JC. Retinal cell responses to elevated intraocular pressure: a gene array comparison between the whole retina and retinal ganglion cell layer. *Invest Ophthalmol Vis Sci*. 2010;51:3003–3018.
5. Butowt R, Jeffrey PL, von Bartheld CS. Purification of chick retinal ganglion cells for molecular analysis: combining retrograde labeling and immunopanning yields 100% purity. *J Neurosci Methods*. 2000;95:29–38.
6. Meyer-Franke A, Kaplan MR, Pfrieger FW, Barres BA. Characterization of the signaling interactions that promote the

survival and growth of developing retinal ganglion cells in culture. *Neuron*. 1995;15:805–819.

7. Lagrèze WA, Pielen A, Steingart R, et al. The peptides ADNF-9 and NAP increase survival and neurite outgrowth of rat retinal ganglion cells in vitro. *Invest Ophthalmol Vis Sci*. 2005;46:933–938.
8. McKernan DP, Cotter TGA. Critical role for Bim in retinal ganglion cell death. *J Neurochem*. 2007;102:922–930.
9. Puliafito CA, Steinert RF, Deutsch TF, Hillenkamp F, Dehm EJ, Adler CM. Excimer laser ablation of the cornea and lens. Experimental studies. *Ophthalmology*. 1985;92:741–748.
10. Trokel SL, Srinivasan R, Braren B. Excimer laser surgery of the cornea. *Am J Ophthalmol*. 1983;96:710–715.
11. Reynolds A, Moore JE, Naroo SA, Moore CBT, Shah S. Excimer laser surface ablation—a review. *Clin Experiment Ophthalmol*. 2010;38:168–182.
12. Biermann J, Grieshaber P, Goebel U, et al. Valproic acid-mediated neuroprotection and regeneration in injured retinal ganglion cells. *Invest Ophthalmol Vis Sci*. 2010;51:526–534.
13. Vandesompele J, De Preter K, Pattyn F, et al. Accurate normalization of real-time quantitative RT-PCR data by geometric averaging of multiple internal control genes. *Genome Biol*. 2002;3:RESEARCH0034.
14. Herdegen T, Bastmeyer M, Bähr M, Stuermer C, Bravo R, Zimmerman M. Expression of JUN, KROX, and CREB transcription factors in goldfish and rat retinal ganglion cells following optic nerve lesion is related to axonal sprouting. *J Neurobiol*. 1993;24:528–543.
15. Schlamp CL, Johnson EC, Li Y, Morrison JC, Nickells RW. Changes in Thy1 gene expression associated with damaged retinal ganglion cells. *Mol Vis*. 2001;7:192–201.
16. Huang W, Fileta J, Guo Y, Grosskreutz CL. Downregulation of Thy1 in retinal ganglion cells in experimental glaucoma. *Curr Eye Res*. 2006;31:265–271.
17. Ohlsson M, Mattsson P, Svensson M. A temporal study of axonal degeneration and glial scar formation following a standardized crush injury of the optic nerve in the adult rat. *Restor Neurol Neurosci*. 2004;22:1–10.